Modelling of the permeability evolution of coal due to sorption

François Bertrand

Supervised by Prof. Olivier Buzzi (UoN)
and Dr Frédéric Collin (ULiege)

July 13^{th} 2018

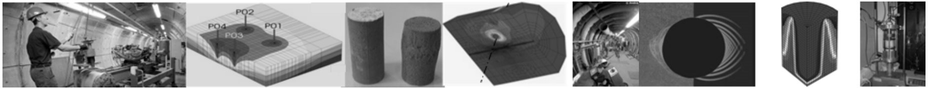

Introduction

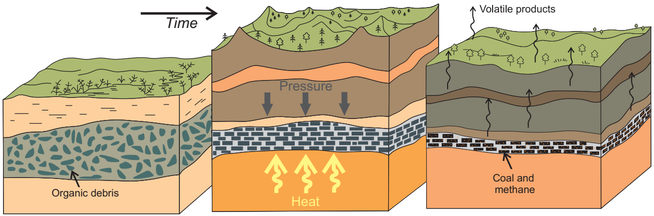

Introduction

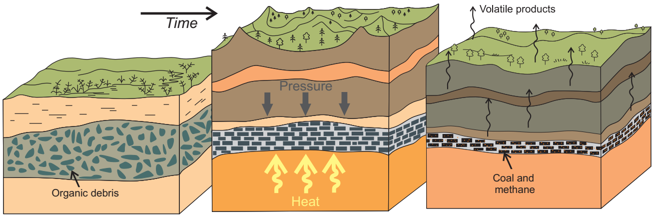

Coalbed methane (CBM)

=

unconventional resource

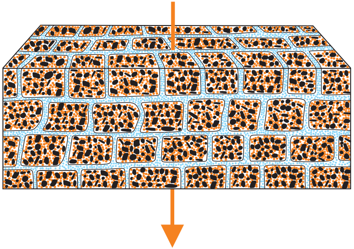

Introduction

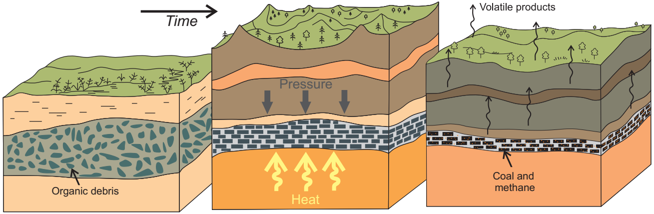

Coalbed methane (CBM)
=
unconventional resource

2 distinct **phenomena affecting permeability**:

- Pressure depletion → **Reservoir compaction** → Cleat permeability ↘
- Gas desorption → Coal **matrix shrinkage** → Cleat permeability ↗

[Gray et al., 1987]

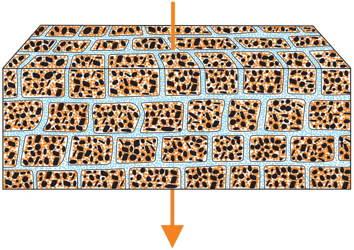

➡ **Unconventional models**

Microscale Model

Tomography imaging

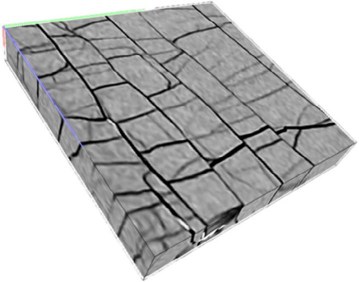

[Jing et al., 2016]

Tomography imaging

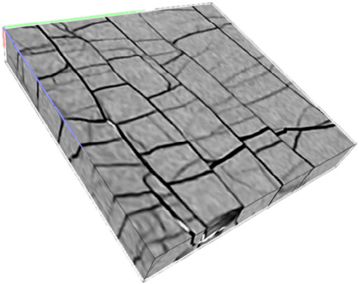

[Jing et al., 2016]

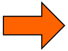

Direct Modelling

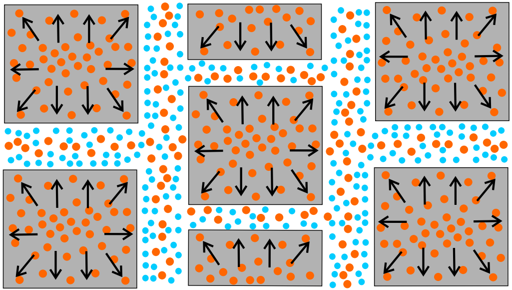

Tomography imaging

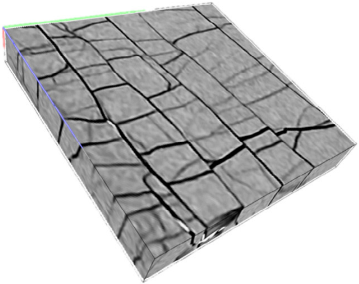

[Jing et al., 2016]

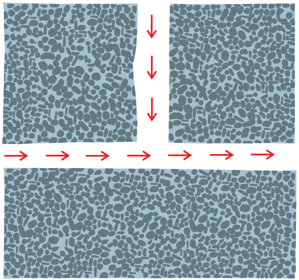

Cleat permeability alteration due to sorption

Navier-Stokes between two parallel plates

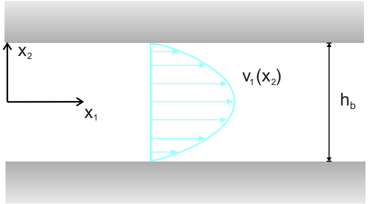

(Laminar flow, Steady state conditions & No body force)

Non-slip boundary conditions at the walls:

$$v\left(x_2 = \pm\frac{h_b}{2}\right) = 0$$

$$\Rightarrow \quad v_1(x_2) \quad = \quad \text{Parabolic profile}$$

$$q = \langle v_1 \rangle = \frac{1}{h_b}\int_{-\frac{h_b}{2}}^{\frac{h_b}{2}} v_1\, dx_2 = -\frac{h_b^2}{12}\cdot\frac{1}{\mu}\frac{dp}{dx_1} \Rightarrow$$ **Darcy permeability** $k = \frac{h_b^2}{12}$

+ Relative permeability curves to take into account **multi-phases flow** (retention curve required)

Microscale Model

Fracture aperture

Darcy permeability $k = \frac{h_b^2}{12}$

The **hydraulic aperture** (h_b) is related to the **mechanical aperture** (h) as:

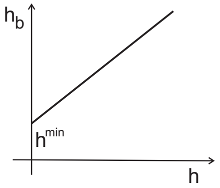

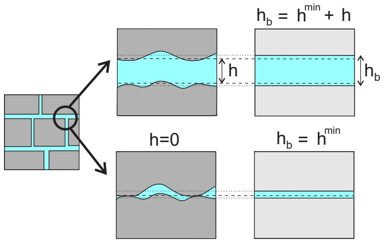

Modified from [Marinelli et al., 2016]

Microscale Model

Fracture aperture

Variation of the **stress state** ($\dot{\sigma}'$) impacts the mechanical **fracture aperture** (h):

$$\dot{h}_{(x)} = \frac{\dot{\sigma}'_{(xx)}}{K_{n_{(x)}}}$$

The **hydraulic aperture** (h_b) is related to the **mechanical aperture** (h) as:

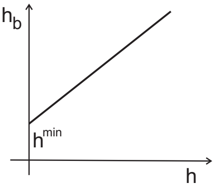

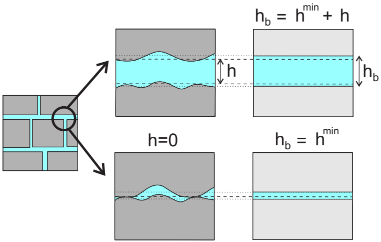

Modified from [Marinelli et al., 2016]

Variation of the **stress state** ($\dot{\sigma}'$) impacts the mechanical **fracture aperture** (h):

$$\dot{h}_{(x)} = \frac{\dot{\sigma}'_{(xx)}}{K_{n_{(x)}}}$$

where K_n is the **normal stiffness** of the fracture:

$$K_n = \frac{K_n^0}{\left(1 - \frac{h_0 - h}{h_0}\right)^2}$$

[Goodman, 1976] & [Bandis et al., 1983]

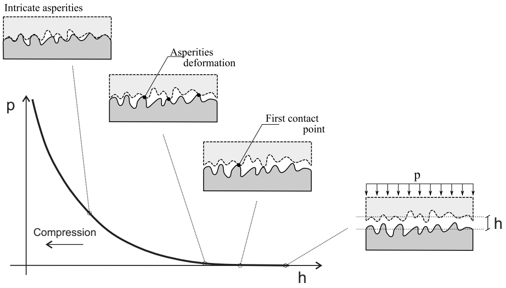

Modified from [Cerfontaine et al., 2015]

A **swelling/shrinkage** of the matrix is induced by the **sorption/desorption**

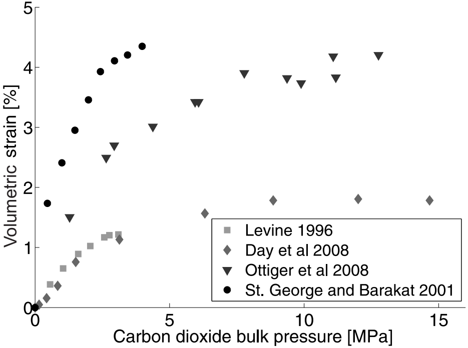

Volumetric **sorption-strain** in the matrix assumed proportional to the **adsorbed gas content** [Cui and Bustin, 2005]:

$$\varepsilon_{vs} = \beta_\varepsilon \cdot V_{g,Ad}$$

$$\Rightarrow \quad \dot{\varepsilon}_{xx_{tot}} = \dot{\varepsilon}_{xx} + \dot{\varepsilon}_{xx_s}$$

Constitutive mechanical model for the matrix:
Isotropic elastic law (2 parameters: e.g. E_m, ν_m)

Microscale Model

Adsorbed gas content

The **adsorbed gas content** in the matrix $V_{g,Ad}$ depends on the pressure in the cleats p

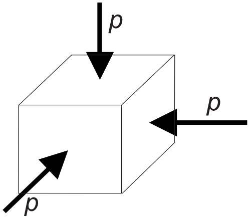

The **adsorbed gas content** in the matrix $V_{g,Ad}$ depends on the pressure in the cleats p

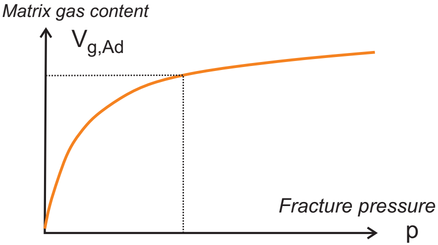

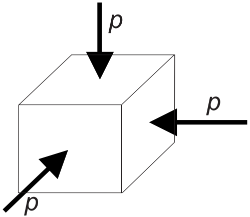

Langmuir's isotherm (equilibrium equation):

$$V_{g,Ad} = \frac{V_L \cdot p}{P_L + p} [m^3/t]$$

[Langmuir, 1918]

Transversal flow (Matrix $\leftrightarrow$ Cleat) $\propto p_{Ad}^{b} - p_{Ad}$

Gas diffusion in the matrix (Fick's law) $\propto \nabla p_{Ad}$

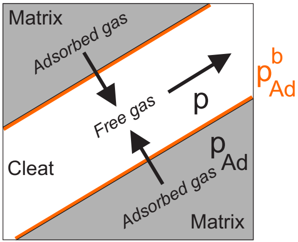

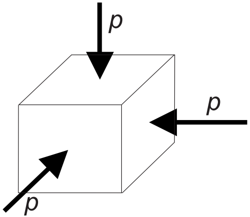

Langmuir's isotherm (equilibrium equation):

$$V_{g,Ad} = \frac{V_L \cdot p}{P_L + p} [m^3/t] \quad \rightarrow \quad p_{Ad}^{b}$$

[Langmuir, 1918]

Microscale Model

Summary

- Matrix
  - Mechanical model

    Isotropic elastic law: E_m, ν_m
  - Hydraulic model

    Fick's diffusion law: D_m^g
  - Hydro-mechanical coupling

    Sorption strain: β_ε

Microscale Model

Summary

- Matrix
  - Mechanical model

    Isotropic elastic law: E_m, ν_m
  - Hydraulic model

    Fick's diffusion law: D_m^g
  - Hydro-mechanical coupling

    Sorption strain: β_ε

- Cleats
  - Mechanical model

    (Stick state) $K_n(h), K_s$

    (Slip state) $+c, \mu$
  - Hydraulic model

    Darcy's law with $k = \frac{h_b^2}{12}$
  - Hydro-mechanical couplings

    $h_b = h^{min} + h$

    $\dot{M}_g(\dot{h}_b)$

    $\sigma' = \sigma + p$

Microscale Model

Summary

- Matrix
  - Mechanical model

    Isotropic elastic law: E_m, ν_m
  - Hydraulic model

    Fick's diffusion law: D_m^g
  - Hydro-mechanical coupling

    Sorption strain: β_ε

- Cleats
  - Mechanical model

    (Stick state) $K_n(h), K_s$

    (Slip state) $+c, \mu$
  - Hydraulic model

    Darcy's law with $k = \frac{h_b^2}{12}$
  - Hydro-mechanical couplings

    $h_b = h^{min} + h$

    $\dot{M}_g(\dot{h}_b)$

    $\sigma' = \sigma + p$

- Matrix $\rightarrow$ Cleats
  - Hydraulic model

    Langmuir's isotherm V_L, P_L

Model implemented in the **FE Lagamine code**

Laboratory Modelling

Laboratory | **Numerical modelling**

- Tomography imaging → Geometry
- Triaxial tests → Mechanical parameters
- Adsorption test → Langmuir 's parameters
- Swelling test → Swelling strain coefficient
- Permeability test → **Permeability evolution**

Geometry, Mechanical parameters, Langmuir 's parameters, Swelling strain coefficient } Model **calibration**

Permeability evolution ← Model **validation**

Objective = **validation of the microscale model**
by comparison between the prediction of the evolution of the permeability and its measurement.

Swelling test

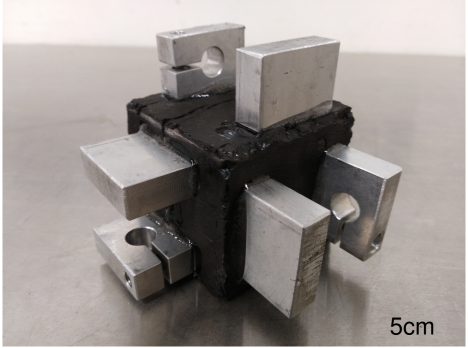

Boundary conditions and loading:

- **Free displacements**
- **Gas pressure increased by steps** (imposed dof)
- Corresponding **total stress applied** (imposed force)

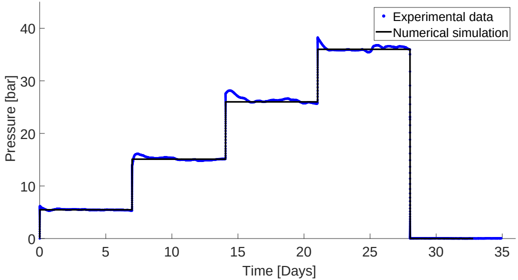

Model calibration

Evolution of the volumetric strain with time

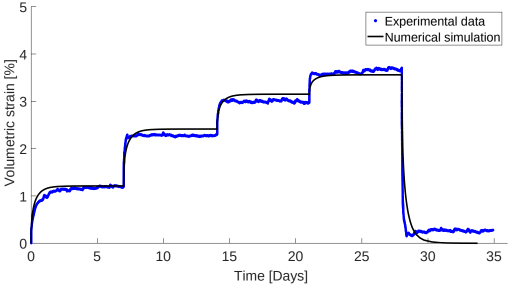

Model calibration

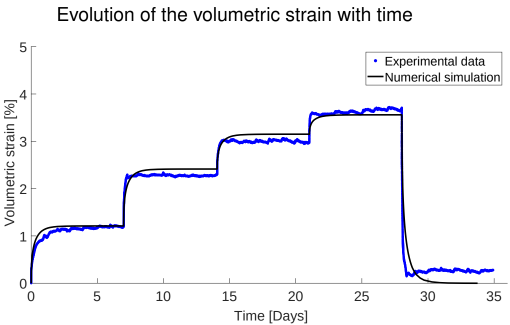

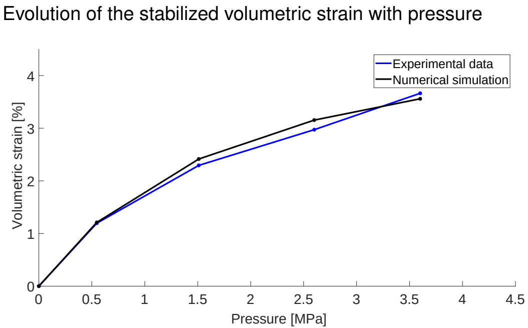

Permeability test

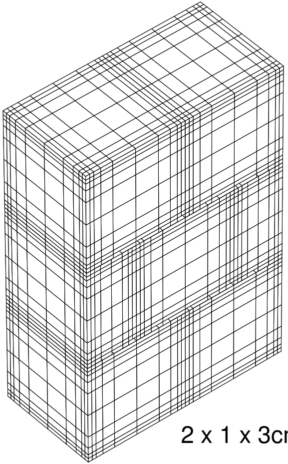

2 x 1 x 3cm

Boundary conditions and loading:

- **Constant volume** (fixed boundaries)
- Constant gas pressure at the top (fixed dof)
- **Gas pressure increased** by steps at the **bottom**

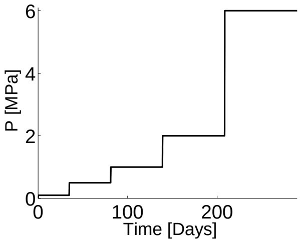

Laboratory Modelling

Permeability test

Adsorbed pressure [Pa]

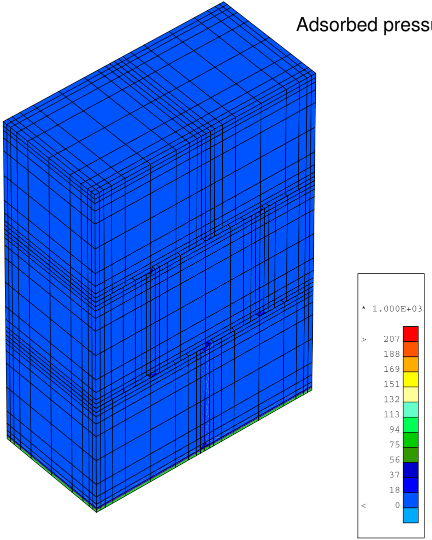

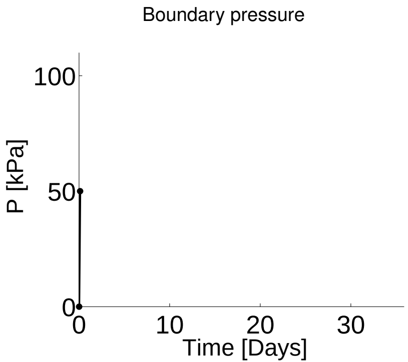

Adsorbed pressure [Pa]

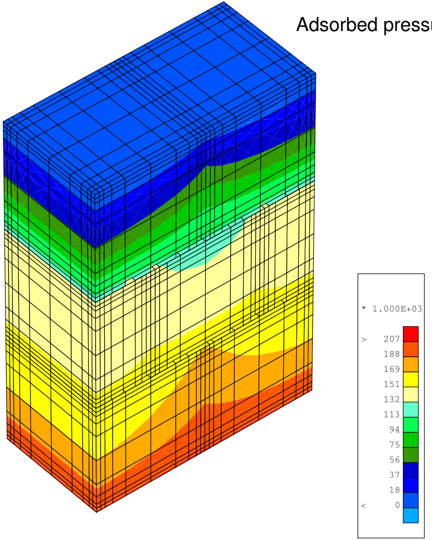

Swelling + Constant volume

Fracture **closure**

Laboratory Modelling

Permeability test

Fracture **aperture evolution**

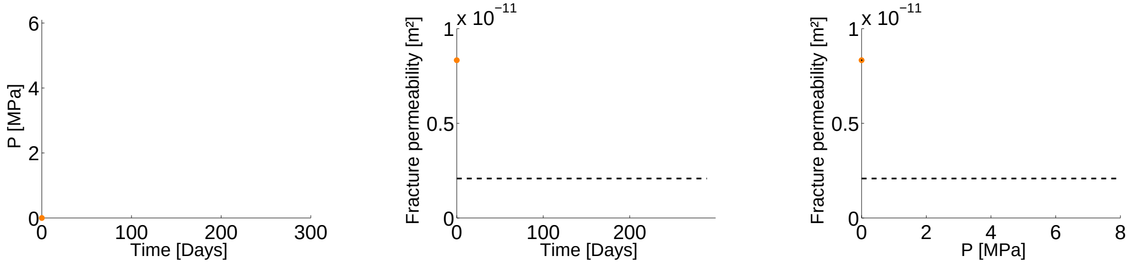

Fracture **permeability evolution**

Development of a numerical **model** at the **scale** of the **fractures** and **matrix blocks**

⇓

Being validated by an experimental laboratory campaign

As is, the model **only usable for laboratory tests** modelling (due to computational expense)

⇒ What about the **reservoir scale**?

Macroscale model

Homogenization

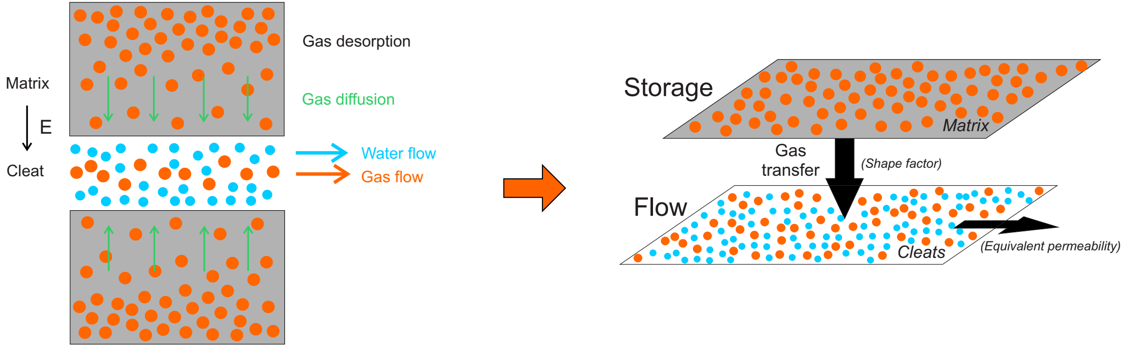

Mass exchange matrix $\rightarrow$ cleats :

$$E = \frac{1}{\tau}\frac{M_g}{RT}\left(p_{g,m} - p_{g,m}^{lim}\right)$$

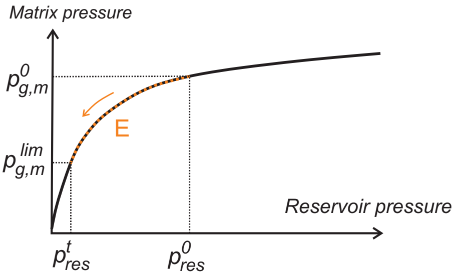

Sorption time:

$$\tau = \frac{1}{\Psi D_m^g}$$

- Diffusion coefficient in the matrix D_m^g
- Shape factor $\Psi(w)$

$$\Psi = \pi^2\left(\frac{1}{w_1^2} + \frac{1}{w_2^2} + \frac{1}{w_3^2}\right)$$

[Lim and Aziz, 1995]

Mass exchange matrix → cleats :

$$E = \frac{1}{\tau}\frac{M_g}{RT}\left(p_{g,m} - p_{g,m}^{lim}\right)$$

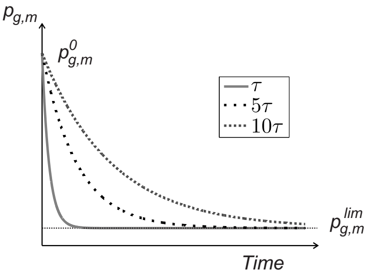

Sorption time:

$$\tau = \frac{1}{\Psi D_m^g}$$

- Diffusion coefficient in the matrix D_m^g
- Shape factor $\Psi(w)$

$$\Psi = \pi^2\left(\frac{1}{w_1^2} + \frac{1}{w_2^2} + \frac{1}{w_3^2}\right)$$

[Lim and Aziz, 1995]

Macroscale model

Hydraulic equivalent medium

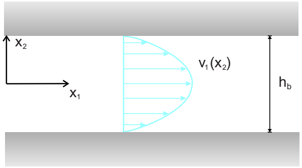

Permeability

Homogenization

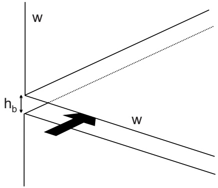

$$k = \frac{h_b^2}{12}$$

$$\boxed{k = \frac{h_b^3}{12w}}$$

$$\dot{\sigma}_{ij} = C_{ijkl}\,\dot{\varepsilon}_{kl}$$

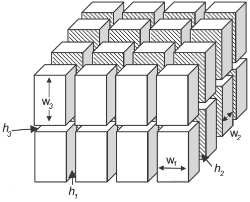

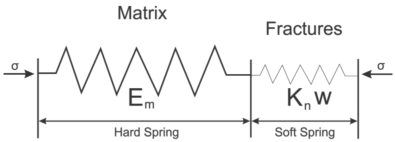

$$\frac{1}{E_x} = \frac{1}{E_m} + \frac{1}{K_{n_x} \cdot w_x}$$

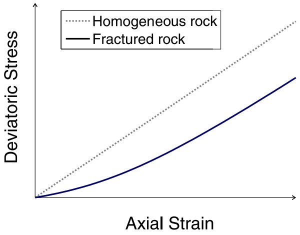

$$K_n = \frac{K_n^0}{\left(1 - \frac{h_0 - h}{h_0}\right)^2}$$

$h \searrow K_n \nearrow$

[Bandis et al., 1983]

- Isotropic elastic matrix: E_m, ν_m
- Nonlinear elastic fractures: K_n, K_s

→ **Orthotropic nonlinear elastic** equivalent medium

Horseshoe Canyon case (Dry reservoir) [Gerami et al., 2007]

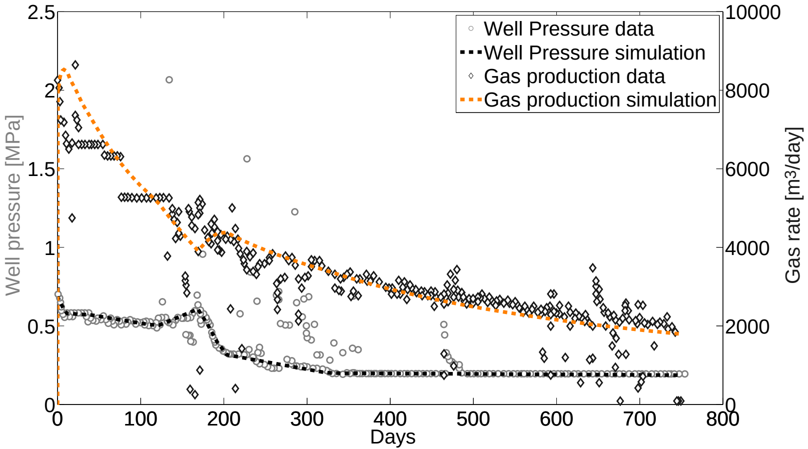

Consistent macroscale model enriched with microscale aspects

[Bertrand et al., 2017]

Remarkable features:

- **Dual-continuum** approach for both mechanical and hydraulic behaviours.
- Not instantaneous gas desorption from the matrix.
- Kinetics of the gas transfer based on **shape factor** and **Langmuir**'s isotherm.
- **Desorption strain** not necessarily fully converted into a fracture opening.
- **Permeability evolution** directly linked to the fracture aperture.
- **Multiphase** flows in the fractures.

But could we go further **avoiding macroscale laws**?

Multiscale Model

FE^2 approach

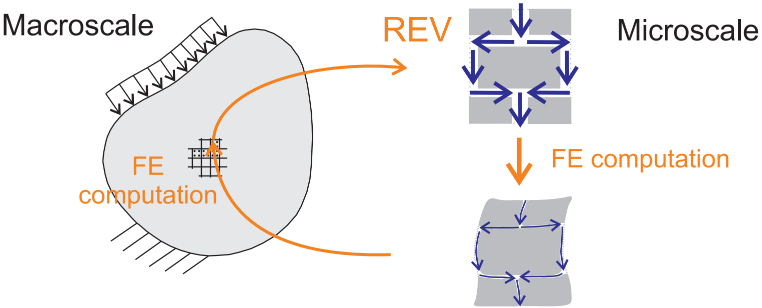

1. Localization
2. Microscale BVP
3. Homogenization
4. Macroscale BVP

Conclusions

Microscale

Highly accurate but **computationally expensive**

→ Laboratory modelling only

Macroscale

Suitable for reservoir modelling but **less accurate**

Multiscale

→ **Compromise** solution

Thank you for your attention!

Modelling of the permeability evolution of coal due to sorption

Researches supported by the FNRS - FRIA and the WBI

FNRS LA LIBERTÉ DE CHERCHER

Wallonie - Bruxelles International.be

References

References I

Bandis, S., Lumsden, A., and Barton, N. (1983).
Fundamentals of rock joint deformation.
In *International Journal of Rock Mechanics and Mining Sciences & Geomechanics Abstracts*, volume 20, pages 249–268. Elsevier.

Bertrand, F., Cerfontaine, B., and Collin, F. (2017).
A fully coupled hydro-mechanical model for the modeling of coalbed methane recovery.
Journal of Natural Gas Science and Engineering, 46:307–325.

Brooks, R. H. and Corey, A. T. (1964).
Hydraulic properties of porous media and their relation to drainage design.
Transactions of the ASAE, 7(1):26–0028.

Cerfontaine, B., Dieudonné, A.-C., Radu, J.-P., Collin, F., and Charlier, R. (2015).
3d zero-thickness coupled interface finite element: formulation and application.
Computers and Geotechnics, 69:124–140.

References II

Coppens, P. L. (1967).
Synthèse des propriétés chimiques et physiques des houilles.
Institut National de l'Industrie Charbonnière.

Cui, X. and Bustin, R. M. (2005).
Volumetric strain associated with methane desorption and its impact on coalbed gas production from deep coal seams.
Aapg Bulletin, 89(9):1181–1202.

Gerami, S., Darvish, M. P., Morad, K., Mattar, L., et al. (2007).
Type curves for dry cbm reservoirs with equilibrium desorption.
In *Canadian International Petroleum Conference*. Petroleum Society of Canada.

Goodman, R. E. (1976).
Methods of geological engineering in discontinuous rocks.

Gray, I. et al. (1987).
Reservoir engineering in coal seams: Part 1-the physical process of gas storage and movement in coal seams.
SPE Reservoir Engineering, 2(01):28–34.

Jing, Y., Armstrong, R. T., Ramandi, H. L., and Mostaghimi, P. (2016).
Coal cleat reconstruction using micro-computed tomography imaging.
Fuel, 181:286–299.

Kundt, A. and Warburg, E. (1875).
Ueber reibung und wärmeleitung verdünnter gase.
Annalen der Physik, 232(10):177–211.

Langmuir, I. (1918).
The adsorption of gases on plane surfaces of glass, mica and platinum.
Journal of the American Chemical society, 40(9):1361–1403.

References IV

- Lim, K. and Aziz, K. (1995).
  Matrix-fracture transfer shape factors for dual-porosity simulators.
  Journal of Petroleum Science and Engineering, 13(3):169–178.
- Marinelli, F., Van den Eijnden, A., Sieffert, Y., Chambon, R., and Collin, F. (2016).
  Modeling of granular solids with computational homogenization: Comparison with biot' s theory.
  Finite Elements in Analysis and Design, 119:45–62.
- Mualem, Y. (1976).
  A new model for predicting the hydraulic conductivity of unsaturated porous media.
  Water resources research, 12(3):513–522.
- Peaceman, D. W. et al. (1978).
  Interpretation of well-block pressures in numerical reservoir simulation (includes associated paper 6988).
  Society of Petroleum Engineers Journal, 18(03):183–194.

References V

- Seidle, J., Jeansonne, M., Erickson, D., et al. (1992).
  Application of matchstick geometry to stress dependent permeability in coals.
  In *SPE rocky mountain regional meeting*. Society of Petroleum Engineers.
- Yuster, S. et al. (1951).
  Theoretical considerations of multiphase flow in idealized capillary systems.
  In *Proceedings of the 3rd World Petroleum Congress, Section II, The Hague*, volume 2, pages 437–445.

Microscale

Triaxial/UCS test

Parameters		Values
Matrix		
Density	ρ_c (kg/m^3)	1500
Young's modulus	E_m (Pa)	3E9
Poisson's ratio	ν_m	0.3
Width	w (m)	0.01
Cleat		
Initial normal stiffness	K_n^0 (Pa/m)	0.01E12
Shear stiffness	K_s (Pa/m)	0.2E12
Friction coefficient	μ	0.57
Cohesion	c (Pa)	1
Initial mechanical aperture	h_0 (m)	50E-6

Swelling & Permeability tests

Parameters		Values
Matrix		
Langmuir volume	V_L (m^3/kg)	0.02
Langmuir pressure	P_L (Pa)	1.5E6
Swelling coefficient	β_ε (kg/m^3)	0.5
Density	ρ_c (kg/m^3)	1500
Young's modulus	E_m (Pa)	3E9
Poisson's ratio	ν_m	0.3
Width	w (m)	0.01
Diffusion coefficient	D_m^g (m^2/s)	1E-11
Cleat		
Initial normal stiffness	K_n^0 (Pa/m)	1E12
Shear stiffness	K_s (Pa/m)	0.2E12
Friction coefficient	μ	0.57
Cohesion	c (Pa)	1
Initial hydraulic aperture	h_0 (m)	10E-6
Minimal hydraulic aperture	h_b^{min} (m)	5E-6

Mechanical problem

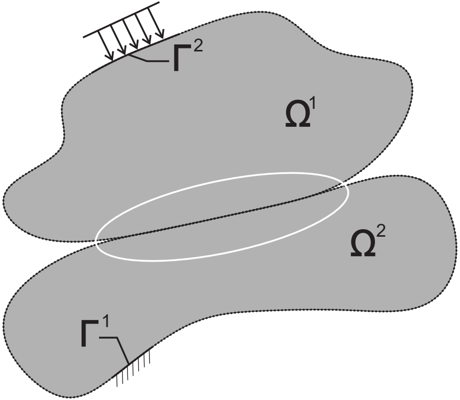

$$\sum_{k=1}^{2}\left[\int_{\Omega^k} \sigma_{ij}\,\frac{\partial v_i^*}{\partial x_j}\,d\Omega\right] = \sum_{k=1}^{2}\left[\int_{\Gamma^k_{\bar{t}_i}} \bar{t}_i\, v_i^*\,d\Gamma + \int_{\Gamma^k_c} T_i^k\, v_i^*\,d\Gamma\right]$$

Hydraulic problem

Matrix:

$$\frac{\partial}{\partial t}\left(\rho_{g,Ad}\right)+\frac{\partial}{\partial x_i}\left(J_{mi}^{g}\right)=0$$

Cleats:

$$\frac{\partial}{\partial t}\left(\rho_{g,f}\,(1-S_r)\;h_b\right)+\frac{\partial}{\partial x_1}\left(\rho_{g,f}\;h_b\;q_{g\,L}+(1-S_r)\;h_b\;J_{g\,1}^{g}\right)+\frac{\partial}{\partial x_2}\left(\rho_{g,f}\;h_b\;(q_{g\,T}^{1}-q_{g\,T}^{2})\right)=0$$

Hydraulic problem

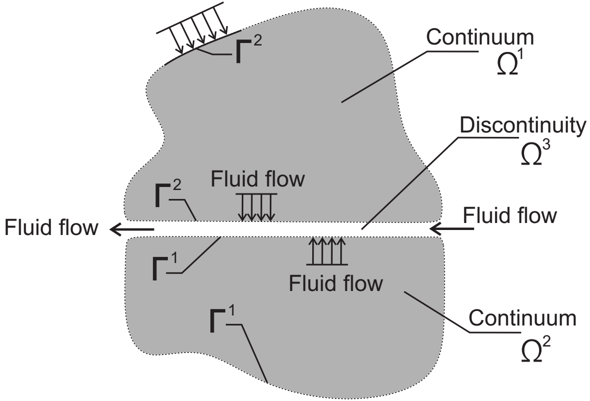

$$\sum_{k=1}^{3}\left[\int_{\Omega^k} \dot{S}_g\, p_g^* - f_{g_i}\frac{\partial p_g^*}{\partial x_i}\, d\Omega\right] = \sum_{k=1}^{3} -\left[\int_{\Gamma^k_{\bar{q}_g}} \bar{q}_g\, p_g^*\, d\Gamma + \int_{\Gamma^k_{\tilde{q}_g}} \tilde{q}_g\, \delta p_g\, d\Gamma\right]$$

Gas slippage?

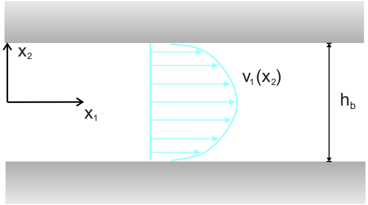

(Laminar flow, Steady state conditions & No body force)

Slip boundary conditions [Kundt and Warburg, 1875]:

$$v_1\left(\frac{h}{2}\right) = -c\bar{l}\,\frac{\mathrm{d}v_1}{\mathrm{d}x_2}\Bigg]_{x_2=\frac{h_b}{2}}$$

$$\Rightarrow\; v_1(x_2) = -\frac{1}{2\mu}\left(c\,\bar{l}\,h_b + \left(\frac{h_b}{2}\right)^2 - x_2^2\right)\frac{\mathrm{d}p}{\mathrm{d}x_1}$$

Gas slippage?

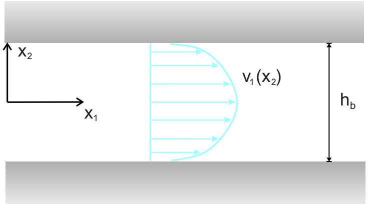

(Laminar flow, Steady state conditions & No body force)

Slip boundary conditions [Kundt and Warburg, 1875]:

$$v_1\left(\frac{h}{2}\right) = -c\bar{l}\,\frac{\mathrm{d}v_1}{\mathrm{d}x_2}\bigg]_{x_2=\frac{h_b}{2}}$$

$$\Rightarrow\ v_1(x_2) = -\frac{1}{2\mu}\left(c\,\bar{l}\,h_b + \left(\frac{h_b}{2}\right)^2 - x_2^2\right)\frac{\mathrm{d}p}{\mathrm{d}x_1}$$

$$q = \langle v_1\rangle = \frac{1}{h_b}\int_{-\frac{h_b}{2}}^{\frac{h_b}{2}} v_1\,dx_2 = -\frac{h_b^2}{12}\left(1+\frac{6c\bar{l}}{h_b}\right)\cdot\frac{1}{\mu}\frac{\mathrm{d}p}{\mathrm{d}x_1}\ \Rightarrow\ k = \frac{h_b^2}{12}\cdot f_c$$

$$f_c = \left(1 + \frac{6c\bar{l}}{h_b}\right)$$

- Constant $c \approx 1$
- **Gas mean free path** $\bar{l}$

$$\bar{l} = \frac{k_B T}{\sqrt{2}\,\pi\, d_g^2\, p}$$

where $p[Pa]$ is the gas **pressure**, d_g the **collision diameter** of the gas molecule, k_B the **Boltzmann** constant and $T[K]$ the **temperature**.

  - $d_g = 380 \cdot 10^{-12} m$ (Methane)
  - $p = 1 MPa$
  - $T = 303K$

$$\rightarrow \quad \bar{l} = 6.52 \cdot 10^{-9} m$$

- **Hydraulic aperture** h_b
  - $h_b = 1 \cdot 10^{-5} m$

$$f_c = \left(1 + \frac{6c\bar{l}}{h_b}\right)$$

- Constant $c \approx 1$
- **Gas mean free path** $\bar{l}$

$$\bar{l} = \frac{k_B T}{\sqrt{2}\,\pi\, d_g^2\, p}$$

where $p[Pa]$ is the gas **pressure**, d_g the **collision diameter** of the gas molecule, k_B the **Boltzmann** constant and $T[K]$ the **temperature**.

  - $d_g = 380 \cdot 10^{-12} m$ (Methane)
  - $p = 1 MPa$
  - $T = 303K$

$$\rightarrow \quad \bar{l} = 6.52 \cdot 10^{-9} m$$

- **Hydraulic aperture** h_b
  - $h_b = 1 \cdot 10^{-5} m$

$$f_c = \left(1 + \frac{6c\bar{l}}{h_b}\right) = 1.004$$

- Constant $c \approx 1$
- **Gas mean free path** $\bar{l}$

$$\bar{l} = \frac{k_B T}{\sqrt{2}\,\pi\, d_g^2\, p}$$

where $p[Pa]$ is the gas **pressure**, d_g the **collision diameter** of the gas molecule, k_B the **Boltzmann** constant and $T[K]$ the **temperature**.

  - $d_g = 380 \cdot 10^{-12} m$ (Methane)
  - $p = 1 MPa$
  - $T = 303 K$

$$\rightarrow \quad \bar{l} = 6.52 \cdot 10^{-9} m$$

- **Hydraulic aperture** h_b
  - $h_b = 1 \cdot 10^{-5} m$

Two-phase flow model?

Integration of Navier-Stokes in each stratum (considering the same velocity at the interface) [Yuster et al., 1951].

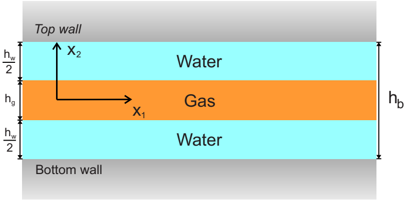

Relative permeabilities:

$$k_{rw} = \frac{S_r^2}{2}(3 - S_r) \qquad k_{rg} = (1 - S_r)^3$$

Saturation degree S_r?

$$s = p_e \cdot (S_r^*)^{\frac{-1}{\lambda}} \quad ?$$

[Brooks and Corey, 1964]

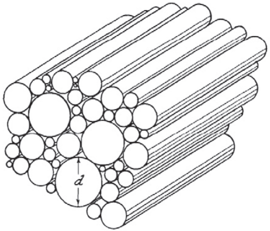

Saturation degree S_r?

$$s = p_e \cdot (S_r^*)^{\frac{-1}{\lambda}} \quad ?$$

[Brooks and Corey, 1964]

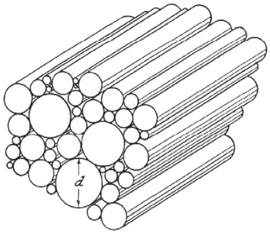

Saturation degree S_r?

Fractal geometry of the wall

$\rightarrow$ Fractal distribution of the number of units N whose radius is larger than r :

$$N(r) = a \cdot r^{-D_f}$$

where $\mathbf{D_f}$ is the **fractal dimension** and a is a constant of proportionality.

$$\rightarrow \quad p_c = p_e \cdot (S_r)^{-\frac{1}{3-D_f}}$$

Saturation degree S_r?

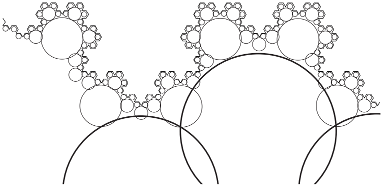

Fractal geometry of the wall

$\rightarrow$ Fractal distribution of the number of units N whose radius is larger than r :

$$N(r) = a \cdot r^{-D_f}$$

where $\mathbf{D_f}$ is the **fractal dimension** and a is a constant of proportionality.

$$\rightarrow \quad p_c = p_e \cdot (S_r)^{-\frac{1}{3-D_f}}$$

Macroscale

Hydraulic model

Mass balance equation

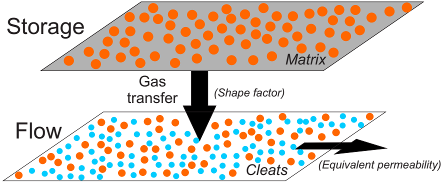

$$\underbrace{\frac{\partial}{\partial t}\left(\rho_{g,f}\,(1-S_r)\phi_f\right)+\frac{\partial}{\partial x_i}\left(\rho_{g,f}\,q_{g\,i}+(1-S_r)\,J^{g}_{g\,i}\right)}_{\text{Gas phase}}$$

$$+\underbrace{\frac{\partial}{\partial t}\left(\rho^{d}_{g,f}\,S_r\phi_f\right)+\frac{\partial}{\partial x_i}\left(\rho^{d}_{g,f}\,q_{l\,i}+S_r\,J^{g}_{l\,i}\right)}_{\text{Dissolved gas in water phase}}=E$$

and $$\frac{\partial}{\partial t}\left(\rho_{g,Ad}\right)=-E$$

Hydraulic model

Matrix - Langmuir's isotherm

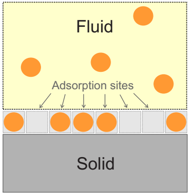

$$\underbrace{G}_{\substack{\text{Gas phase molecules}\\ \propto\, p}} + \underbrace{O-}_{\substack{\text{Vacant adsorption sites}\\ \propto\, 1-\theta}} \rightleftharpoons \underbrace{O-G}_{\substack{\text{Adsorbed gas}\\ \propto\, \theta}}$$

θ: surface coverage of adsorbed molecules

p: pressure of gas

$$K = \frac{[O-G]}{[G]\cdot[O-]} \Rightarrow k = \frac{\theta}{(1-\theta)\cdot p} \Rightarrow \theta = \frac{k\cdot p}{1+k\cdot p}$$

$V_{g,Ad} = \theta \cdot V_L$, where V_L is the monolayer adsorption capacity

$$\Rightarrow V_{g,Ad} = \frac{V_L \cdot p_{res}}{P_L + p_{res}}$$

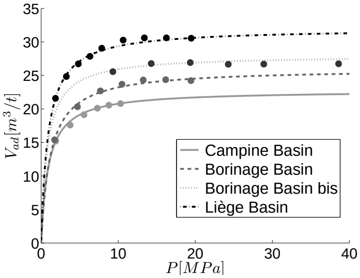

Figure: Data published by [Coppens, 1967].

Hydraulic model

Matrix → Cleats - Analytical solution

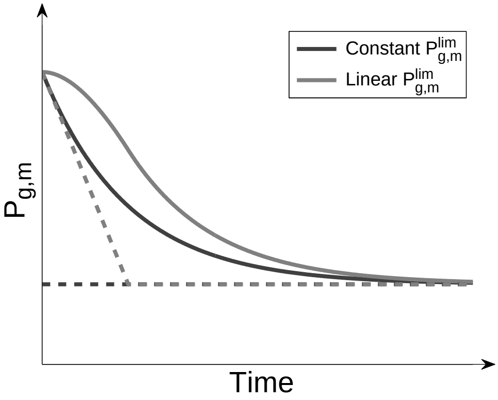

$$\dot{p}_{g,m}(t) = -\frac{1}{\tau} \cdot \left(p_{g,m}(t) - p^{lim}_{g,m}(t)\right)$$

Solution for constant $p^{lim}_{g,m}$:

$$p_{g,m}(t) = \left(p^0_{g,m} - p^{lim}_{g,m}\right) \cdot \exp\left(\frac{-t}{\tau}\right) + p^{lim}_{g,m}$$

Solution for the linear evolution of $p^{lim}_{g,m}$ (slope a) :

$$p_{g,m}(t) = -a\,\tau \exp\left(\frac{-t}{\tau}\right) + a\,(\tau - t) + p^0_{g,m}$$

Hydraulic model

Matrix $\rightarrow$ Cleats - Analytical solution

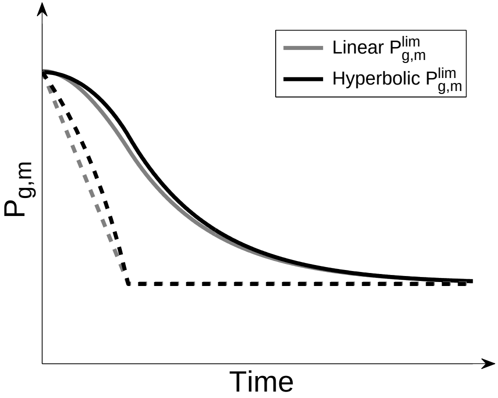

$$\dot{p}_{g,m}(t) = -\frac{1}{\tau} \cdot \left(p_{g,m}(t) - p_{g,m}^{lim}(t)\right)$$

Hyperbolic evolution of $p_{g,m}^{lim}$

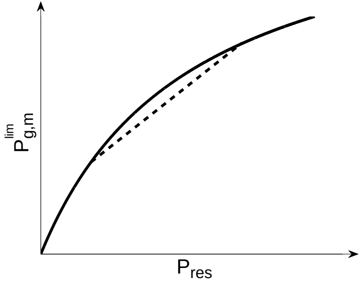

Hydraulic model

Matrix $\rightarrow$ Cleats - Analytical solution

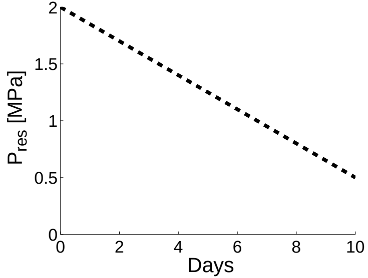

$$V_L = 0.02m^3/kg$$

$$P_L = 1.5MPa$$

$$\tau = 3days$$

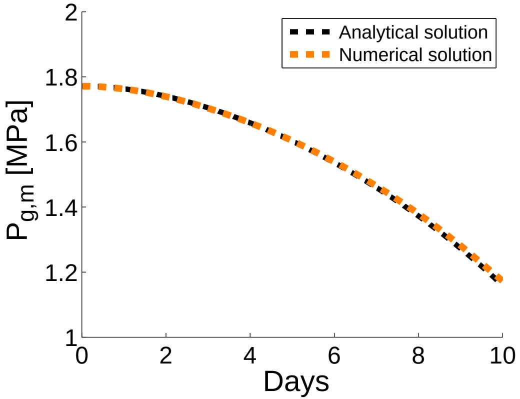

Hydraulic model

Cleats - Permeability change

$$\left(\frac{k}{k_0}\right) = \left(\frac{\phi_f}{\phi_{f_0}}\right)^3$$

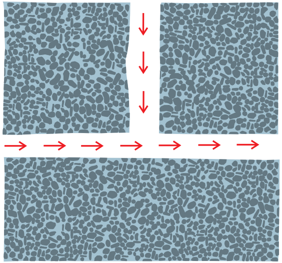

2 distinct phenomena affecting permeability:

- Pressure depletion $\rightarrow$ Reservoir compaction $\rightarrow$ Cleat permeability $\searrow$
- Gas desorption $\rightarrow$ Coal matrix shrinkage $\rightarrow$ Cleat permeability $\nearrow$

$$\phi_f = \phi_{f_0} \exp\{-c_f(\sigma - \sigma_0)\}$$

where c_f is the cleat compressibility.

$$\Rightarrow \; k_f = k_{f_0} \exp\{-3c_f(\sigma - \sigma_0)\}$$

[Seidle et al., 1992]

Hydraulic model

Cleats - Unsaturated conditions

$$k_e = k_r(S_r) \cdot k$$

$$k_{rw} = (S_r^*)^{\eta + 1 + \frac{2}{\lambda}}$$

$$k_{rg} = (1 - S_r^*)^{\eta} \cdot \left[1 - (S_r^*)^{1+\frac{2}{\lambda}}\right]$$

with

$$S_r^* = \frac{S_r - S_{w,res}}{1 - S_{w,res} - S_{g,res}}$$

$$= \frac{S_r - S_{w,res_0}\left(\frac{\phi}{\phi_0}\right)^{-1}}{1 - S_{w,res_0}\left(\frac{\phi}{\phi_0}\right)^{-1} - S_{g,res_0}\left(\frac{\phi}{\phi_0}\right)^{-1}\left(\frac{\rho_g}{\rho_{g0}}\right)^{-1}}$$

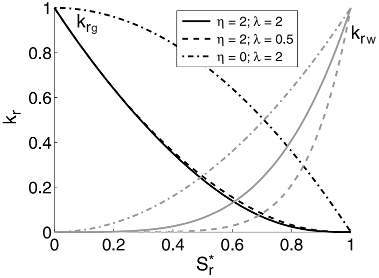

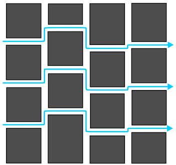

Tortuosity effect η

Cleat density effect λ

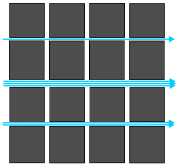

Hydraulic model

Cleats - Unsaturated conditions

$$k_e = k_r(S_r) \cdot k$$

$$k_{rw} = (S_r^*)^\eta \frac{\int_0^{S_r} \frac{dS_r}{s^2}}{\int_0^1 \frac{dS_r}{s^2}}$$ [Mualem, 1976]

$$s = p_e \cdot (S_r^*)^{\frac{-1}{\lambda}}$$

[Brooks and Corey, 1964]

$$k_{rw} = (S_r^*)^{\eta+1+\frac{2}{\lambda}}$$

$$k_{rg} = (1 - S_r^*)^\eta \cdot \left[1 - (S_r^*)^{1+\frac{2}{\lambda}}\right]$$

with
$$S_r^* = \frac{S_r - S_{w,res}}{1 - S_{w,res} - S_{g,res}}$$

$$= \frac{S_r - S_{w,res_0}\left(\frac{\phi}{\phi_0}\right)^{-1}}{1 - S_{w,res_0}\left(\frac{\phi}{\phi_0}\right)^{-1} - S_{g,res_0}\left(\frac{\phi}{\phi_0}\right)^{-1}\left(\frac{\rho_g}{\rho_{g0}}\right)^{-1}}$$

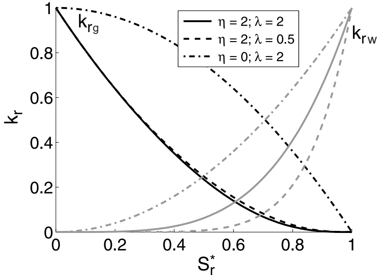

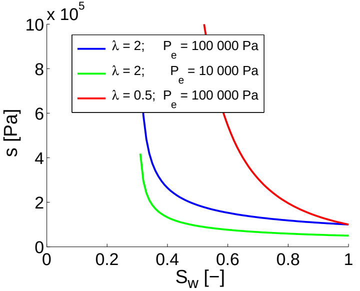

Reservoir modelling

Synthetic reservoir

Well

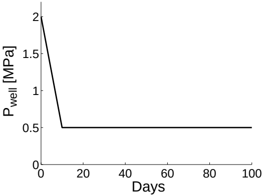

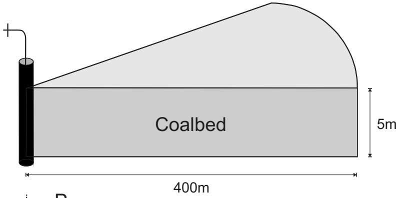

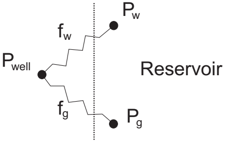

$$f_w = T \cdot \rho_w \cdot \frac{k_{rw}}{\mu_w} \left(P_w - P_{well} \right)$$

$$f_g = T \cdot \rho_g \cdot \frac{k_{rg}}{\mu_g} \left(P_g - P_{well} \right) + H \cdot \rho_g \frac{f_w}{\rho_w}$$

[Peaceman et al., 1978]

Reservoir

Initially in the cleats:

$$P_{w_0} = 2MPa$$

$$P_{g_0} = 2MPa$$

In the matrix:

P_g on the Langmuir's isotherm

Reservoir modelling

Synthetic reservoir - Reference case

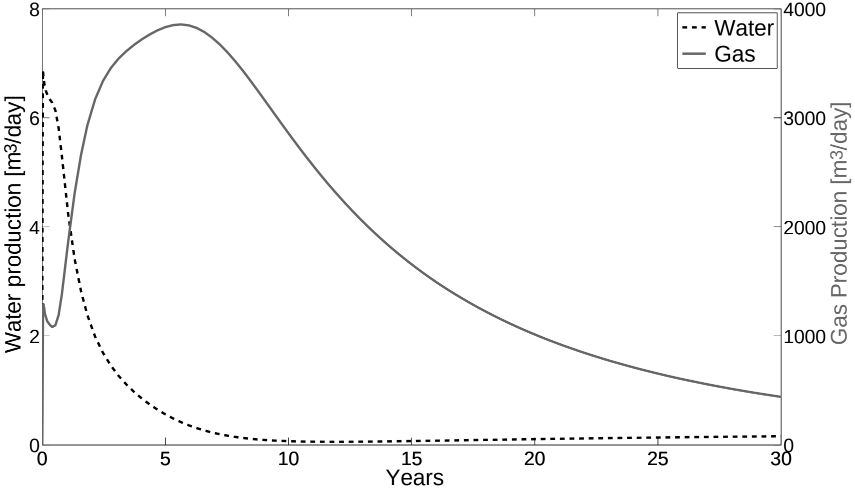

Reservoir modelling

Synthetic reservoir - Production scenario influence

Influence of the depletion rate on the permeability evolution

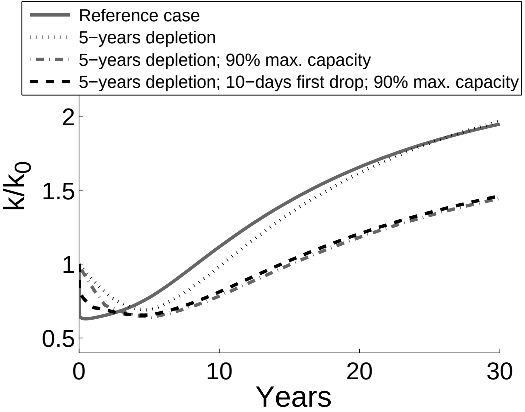

Reservoir modelling

Synthetic reservoir - Production scenario influence

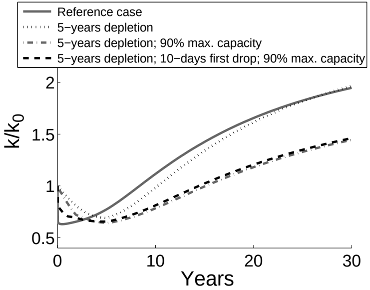

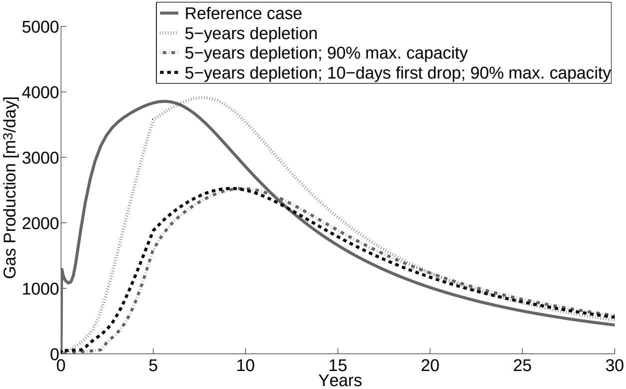

Reservoir modelling

Synthetic reservoir - Production scenario influence

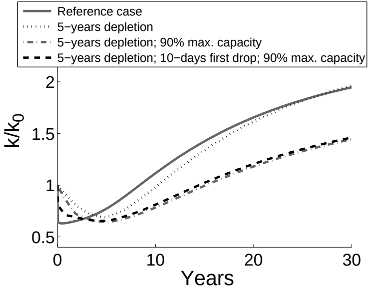

$$p_{res} = 2MPa$$

$$p_{g,m}^{max} = \frac{RT}{M_g} \cdot \rho_{g,std} \cdot \rho_c \cdot \frac{V_L \cdot p_{res}}{P_L + p_{res}} = 1.897\ MPa$$

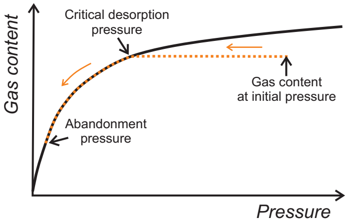

$$p_{res}^{crit} = \frac{0.9 \cdot p_{g,m}^{max} \cdot P_L}{\left(\frac{RT}{M_g} \cdot \rho_{g,std} \cdot \rho_c \cdot V_L - 0.9 \cdot p_{g,m}^{max}\right)} = 1.588\ MPa$$

Reservoir modelling

Synthetic reservoir - Production scenario influence

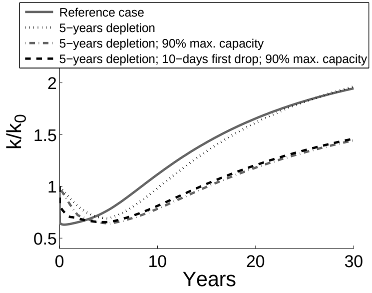

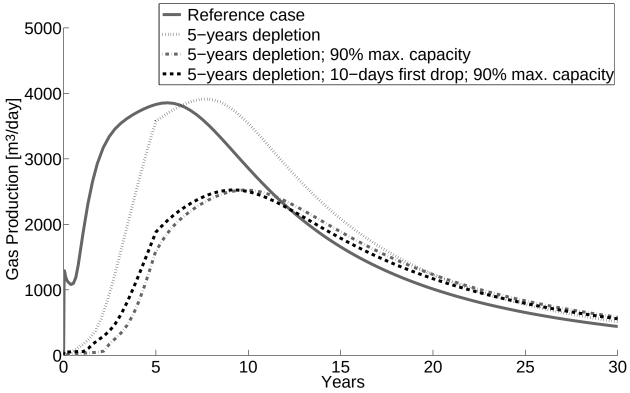

Reservoir modelling

Synthetic reservoir - Reference case parameters

Parameters	Values
Seam thickness (m)	5
Reservoir radius (m)	400
Temperature (K)	303
Overburden pressure (Pa)	5E6
Well transmissibility T (m^3)	1E-12
Penalty coefficient κ ($m^2.s/(kg.Pa)$)	1.5E-19
Coal density ρ_c (kg/m^3)	1500
Matrix Young's modulus E_m (Pa)	5E9
Matrix Poisson's ratio ν_m	0.3
Matrix width w (m)	0.02
Cleat aperture h (m)	2E-5
Cleat normal stiffness K_n (Pa/m)	100E9
Cleat shear stiffness K_s (Pa/m)	25E9
Maximum cleat closure ratio	0.5
Joint Roughness coefficient JRC	0

Synthetic reservoir - Reference case parameters

Parameters	Values
Sorption time τ (days)	3
Langmuir volume V_L (m^3/kg)	0.02
Langmuir pressure P_L (Pa)	1.5E6
Matrix shrinkage coefficient β_ε (kg/m^3)	0.4
Entry capillary pressure p_e (Pa)	10000
Cleat size distribution index λ	0.25
Tortuosity coefficient η	1
Initial residual water saturation S_{r,res_0}	0.1
Residual water saturation exponent, n_{wr}	0.5
Residual gas saturation	0.0

Reservoir modelling

Synthetic reservoir - Parametric and couplings analysis

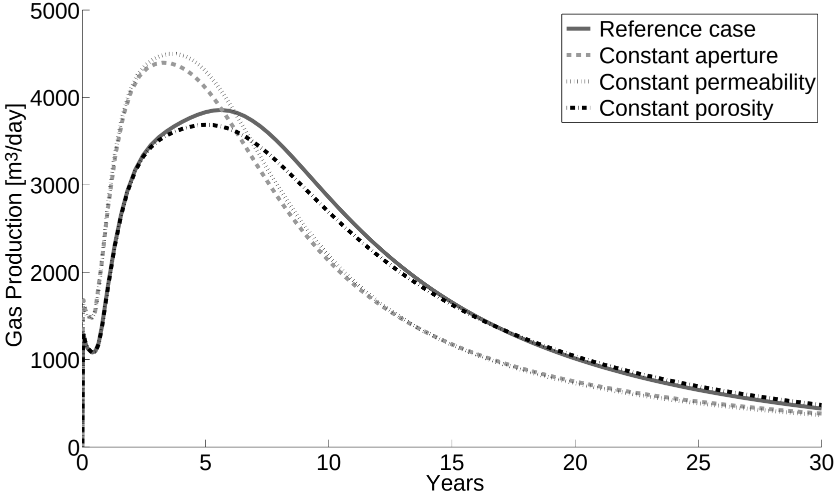

Reservoir modelling

Synthetic reservoir - Parametric and couplings analysis

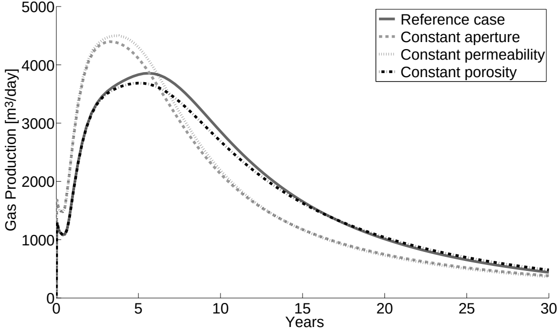

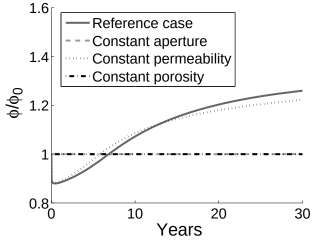

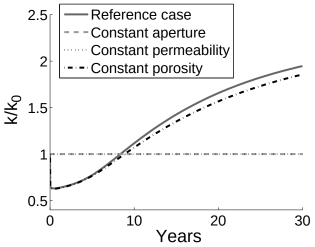

Reservoir modelling

Synthetic reservoir - Parametric and couplings analysis

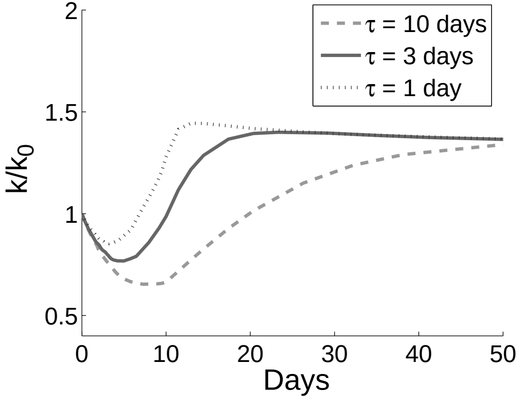

Reservoir modelling

Synthetic reservoir - Parametric and couplings analysis

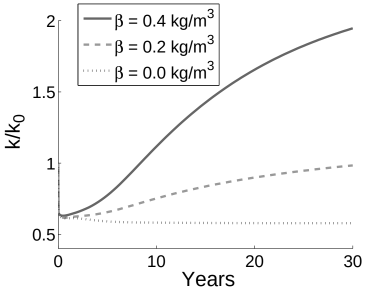

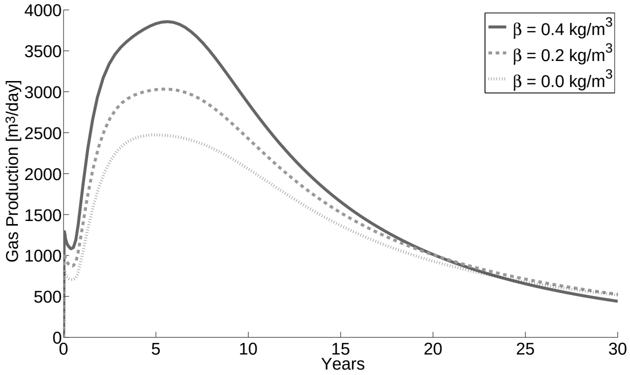

Multiscale

Multiscale model

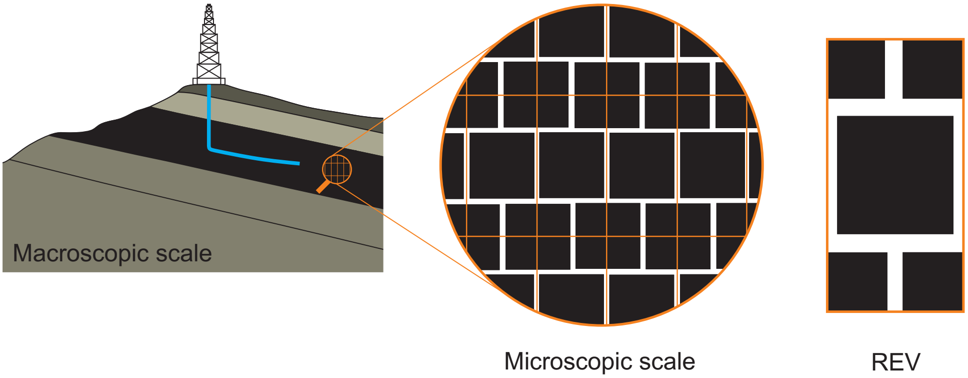

FE^2

1. **Macroscopic structure** discretised by finite elements

2. **Macroscopic deformation gradient tensor** computed for each IP from the estimation of the macroscopic nodal displacements relative to the external load

3. **REV** assigned at each macroscopic IP

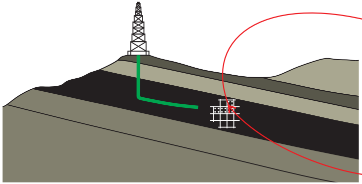

4. **Localization**: apply appropriate **displacements to the REV** from the macroscopic deformation gradient tensor

5. **Microscale FE computation**: stress and deformation distributions in the REV

6. **Homogenization**: REV **averaged stress** returned to the macroscopic IP

7. Macroscopic **internal nodal forces**

8. **Macroscopic stiffness matrix**

9. **Balance** between external load and internal load?

+ **Next time** increment evaluated

– **Updated estimation** of the nodal **displacements** required (via macroscopic stiffness matrix)